

# Bioceramics Composed of Octacalcium Phosphate Demonstrate Enhanced Biological Behavior

Vladimir S. Komlev,<sup>\*,†,‡,§</sup> Sergei M. Barinov,<sup>†</sup> Ilya I. Bozo,<sup>§</sup> Roman V. Deev,<sup>§</sup> Ilya I. Eremin,<sup>||</sup> Alexander Yu. Fedotov,<sup>†</sup> Alex N. Gurin,<sup>‡,⊥,♯</sup> Natalia V. Khromova,<sup>¶</sup> Pavel B. Kopnin,<sup>¶</sup> Ekaterina A. Kuvshinova,<sup>○</sup> Vasily E. Mamonov,<sup>△</sup> Vera A. Rybko,<sup>¶</sup> Natalia S. Sergeeva,<sup>○</sup> Anastasia Yu. Teterina,<sup>†</sup> and Vadim L. Zorin<sup>§</sup>

<sup>†</sup>A.A. Baikov Institute of Metallurgy and Materials Science, Russian Academy of Sciences, Moscow, Russia

<sup>‡</sup>BioNova LLC, Moscow, Russia

<sup>§</sup>Human Stem Cells Institute, Moscow, Russia

<sup>||</sup>State Research Centre—Burnasyan Federal Medical Biophysical Centre, Federal Medical Biological Agency of Russia, Moscow, Russia

<sup>⊥</sup>Central Scientific Research Institute of Dentistry and Maxillofacial Surgery, Moscow, Russia

<sup>♯</sup>I.M. Sechenov First Moscow State Medical University, Moscow, Russia

<sup>¶</sup>Institute of Carcinogenesis, N.N. Blokhin Russian Cancer Research Center, Moscow, Russia

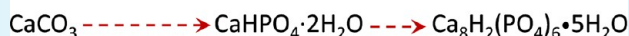
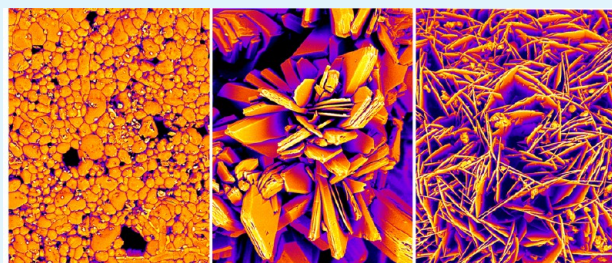
<sup>○</sup>P.A. Herten Moscow Oncology Research Institute, Moscow, Russia

<sup>△</sup>National Hematology Research Centre, Moscow, Russia

## Supporting Information

**ABSTRACT:** Bioceramics are used to treat bone defects but in general do not induce formation of new bone, which is essential for regeneration process. Many aspects related to bioceramics synthesis, properties and biological response that are still unknown and, there is a great need for further development. In the most recent research efforts were aimed on creation of materials from biological precursors of apatite formation in humans. One possible precursor is octacalcium phosphate (OCP), which is believed to not only exhibit osteoconductivity but possess osteoinductive quality, the ability to induce bone formation. Here we propose a relatively simple route for OCP ceramics preparation with a specifically designed microstructure. Comprehensive study for OCP ceramics including biodegradation, osteogenic properties in ortopic and heterotopic models and limited clinical trials were performed that demonstrated enhanced biological behavior. Our results provide a possible new concept for the clinical applications of OCP ceramics.

**KEYWORDS:** octacalcium phosphate, ceramics, bone graft, osteoconductive, osteoinductive, osteotransductive features



## 1. INTRODUCTION

Tissue-defect management relies on auto- or allografting techniques.<sup>1</sup> Synthetic tissue graft substitutes have been developed to avoid the problems posed by the surgically induced morbidity of autologous grafts and by the inherent immunogenicity of allografts. Over the last few decades, a number of calcium phosphate biomaterials have been developed for engineering of artificial bone grafts.<sup>2</sup> Thus, the clinical applications of sintered hydroxyapatite (HA) ceramics—although not so many were used in the replacement of bone defects yet—face an intrinsic limitation because of the low biodegradability and new bone formation rate. A better control of the process of an artificial graft biodegradation and bone substitution was based on the concept of a biphasic HA –

tricalcium phosphate (TCP) ceramic composites or different anion and cation substitutions in apatite.<sup>2,3</sup> However, HA phase remained essentially unaltered at the implantation site throughout the patient's life.<sup>4</sup> The graft was “included” in the repaired bone rather than being “substituted” by newly formed bone matrix. TCP ceramics alone are well-characterized and are reliable, biodegradable commercially available materials.<sup>5–7</sup> However, the biodegradation of TCP materials do not match the parallel rate of bone growth. All of them can be classified as osteoconductive materials. In other words, the major drawback

**Received:** May 26, 2014

**Accepted:** September 3, 2014

**Published:** September 3, 2014

of all these materials is the complete absence of osteoinductivity and therefore, they have been used as scaffold materials in combination with cells, growth factors or gene constructions.

During the last several years, growing attention has been brought to octacalcium phosphate (OCP) as a synthetic bone substitute material.<sup>8–11</sup> OCP have been proposed a possible precursor of the tooth enamel, dentine and bones in living organisms.<sup>2</sup> The approaches aimed to test properties of various OCP phase compositions that were as close to the earliest steps of natural bone tissue growth as possible with a hope for a significant improvement of its biological behavior. It has been previously reported that OCP pressed powders had osteoconductive property when implanted in the subperiosteal region of mouse calvaria.<sup>12,13</sup> Further, it has been demonstrated that OCP-based materials could stimulate osteoblastic cell differentiation *in vitro*<sup>9,10,14</sup> and had the capacity to provide new bone formation *in vivo*.<sup>15–19</sup> Only recently, the first limited clinical application of OCP/collagen composite in bone defect replacement was reported. This study demonstrated that OCP/collagen composite could be used safely and that it enhanced bone regeneration in human bone defects.<sup>20</sup>

It is very important to note that all of the studies mentioned above were carried out with OCPs that were prepared by lightly grinding of the pressed dried OCP powders. In particular, the first clinical experience work was performed with OCP/collagen composite because OCP material could not be molded using sintering processes. To resolve the disadvantages, including the improvement of handling, OCP was combined with collagen (OCP/collagen).<sup>20</sup> Therefore, the obtained agglomerates of OCP powders did not form an architecture required for artificial bone grafts. The most successful formulation was reported by Suzuki et al.<sup>12</sup> and by Murakami et al.<sup>19</sup> Briefly, the granules, consisting of OCP crystal aggregates, were prepared by light grinding using a pestle and mortar of the dried OCP cake after the chemical synthesis and then passing through a standard testing sieve.<sup>19</sup> The problem is that OCP is thermodynamically unstable material; therefore it is impossible to apply traditional ceramic technologies such as high temperature treatment.

In this study, we demonstrated the use of a relatively simple processing route based on preparation of calcium carbonated (CC) ceramics through high temperature treatment with designed controlled microstructure followed by chemical transformation of these ceramics into octacalcium phosphate material by treatment in chemical solutions. Granules as the most appropriate formulation were used as a model. We further performed a comprehensive study of OCP ceramics including biodegradation, the osteogenic properties in ortopic and heterotopic models and the contemporary bone deposition after *in vivo* implantation, which showed that the obtained material did not satisfy the definitions “osteoconductivity” and “osteoinductivity”. Finally, an explicit new methodology for bone production was transferred directly to a pilot clinical trial. Two clinical cases are described in this manuscript.

## 2. EXPERIMENTAL SECTION

**2.1. Chemicals and Reagents.** Octacalcium phosphate granules were prepared from calcium carbonate powders. The reagents were purchased from Sigma-Aldrich: high-purity-grade calcium oxide (Cat. No: 1305–78–8), ammonium carbonates (Cat. No: 506–87–6), ammonium phosphate monobasic (Cat. No: 7722–76–1), potassium carbonate–sodium carbonate mixture (Cat. No: 10424–09–6), sodium acetate (Cat. No: 127–09–3), gelatin (Cat. No: 9000–70–8).

**2.2. Preparation of OCP Ceramic Granules.** For synthesis of starting calcium carbonate powders, 30 g of CaO, 62 g of  $(\text{NH}_4)_2\text{CO}_3$ , and 300 mL of distilled water was added to a vessel for grinding. Grinding was carried out for 30 min at room temperature. After filtration, powders were washed and dried at 80 °C for 24 h. Calcium carbonate granules were prepared according to the method described elsewhere.<sup>21</sup> The method is based on liquids immiscibility effect using the powder/gelatin suspension and oil as liquids. The granules of diameter ranging from 50 to 2000  $\mu\text{m}$  were produced. Briefly, 100 mL of 10% gelatin solution was added 50 g of calcium carbonate and stirred for 30 min at 60 °C. The granules were filtered, dried and sintered at 650 °C using a sintering additive.<sup>22</sup> Then the calcium carbonate ceramic granules were transformed to octacalcium phosphate as described elsewhere.<sup>23</sup> An aqueous solution was prepared by dissolving of 115 g of  $\text{NH}_4\text{H}_2\text{PO}_4$  in 500 mL of distilled water at room temperature, pH  $4.1 \pm 0.1$ . Ten grams ( $\pm 1$  g) of calcium carbonate granules were added to the solution. The granules were shaken in a sealed glass vessel for 168 h at 40 °C. After that the granules were thoroughly washed in distilled water at least 5 times and dried overnight at 37 °C. The obtained granules in amounts of  $10 \pm 1$  g were placed in a second solution. Briefly, the second solution was prepared by dissolving 95.2 g of  $\text{CH}_3\text{COONa}$  in 700 mL of distilled water at 40 °C and pH  $8.2 \pm 0.2$ . The granules were again shaken in a sealed glass vessel for 168 h at 40 °C. Then they were thoroughly washed in distilled water at least 5 times and dried overnight at 37 °C. The granules with diameter  $500 \pm 100 \mu\text{m}$  were selected using standard sieves and were used for experiments. This size of the granules was chosen according to the work of Murakami et al.<sup>19</sup> The sieved OCP ceramic granules were sterilized by heating at 120 °C for 2 h.<sup>12</sup>

**2.3. Characterization of OCP Ceramic Granules.** The porosity, intergranule size and specific surface area of the investigated materials were determined by mercury porosimetry (TriStar 3000, Micromeritics, USA). The phase composition was analyzed by conventional X-ray diffraction (XRD) technique (Shimadzu XRD-6000, Japan), Ni-filtered  $\text{CuK}\alpha_1$  target,  $\lambda = 1.54183 \text{ \AA}$ . Samples were scanned from  $2\theta = 3^\circ$  to  $60^\circ$  with a step size of  $0.02^\circ$  and a preset time of 5 s. Scanning electron microscopy (SEM) apparatus (Tescan Vega II, Czech Republic), working in secondary and backscattered electron modes, was used for microstructure studies of the ceramic samples. For SEM study the samples were sputter-coated prior to imaging, with a 25 nm-thick gold layer to impart electrical conductivity to the specimen surfaces. Infrared spectroscopy (IR) (Nicolet Avatar 330 FTIR spectrometer, England) was performed after mixing 1 mg of sample with 300 mg of KBr powder followed by compacting those into a thin pellet in a stainless steel die with 1 cm inner diameter. IR data were recorded over the range of  $4000$  to  $400 \text{ cm}^{-1}$  with 128 scans. The solubility of OCP ceramic granules was studied in TRIS-HCl buffer solution at pH 7.4 (according to ISO 10993–14–2001) for 21 days at a constant liquid phase volume (closed system). The buffer solution was adjusted to pH = 7.4 by adding 13.25 g of TRIS (Cat. No: 77–86–1, Sigma-Aldrich) and 125 mL of HCl (Cat. No: 7647–01–0, Aldrich–Aldrich). The solid-to-liquid ratio was 0.5 g/100 mL. The calcium concentration in the liquid phase was measured using an atomic emission spectrometer Ultima 2 (Jobin-Yvon, France).

**2.4. Protein Adsorption Test.** Two proteins solutions were chosen: bovine serum albumin (BSA) (Cat. No: A2058, Sigma-Aldrich) and platelet lysate (PL) prepared from human platelet concentrate. PL was obtained according to a method described elsewhere.<sup>24</sup> Briefly, the platelet concentrate obtained by thrombocytapheresis (Amicus, Fenwal, USA) from 27 male and 19 female donors (mean age 33 years: males 31 years old and women 35 years old) was used for PL preparation. The majority of donors was under 45 years old. PL was prepared by freeze–thawing method, resulting in degradation of  $\alpha$ -granules and release of growth and other biologically active factors: the tubes with the platelet concentrate were frozen at  $-80^\circ\text{C}$  and then rapidly thawed at  $37^\circ\text{C}$ . The content of tubes was transferred to 15 mL plastic tubes and platelet fragments were precipitated by triple centrifugation at 3000 rpm for 30 min (Eppendorf 5810R centrifuge, Germany). Then, the obtained PL

was aliquoted (in crioampules, 500 mkl, Corning, USA) and frozen at  $-80^{\circ}\text{C}$ . Pooled samples of PL were used in experiments. The fraction of OCP ceramics having granular dimensions ranging from 100 to 150  $\mu\text{m}$  was selected for this experiment. 0.5 to 3.0 mg/mL solutions of BSA and PL were prepared in a phosphate-buffered saline (PBS) at pH 7.2. 50 mg of OCP ceramic granules were immersed in purified protein solutions for 20 h at  $22^{\circ}\text{C}$  to saturate binding. Adsorption conditions were selected so that excess protein was still present in a solution at the end of incubation. The amount of protein adsorbed onto that surface of OCP ceramic granules was quantified with the Folin phenol reagent after alkaline copper treatment.<sup>25</sup>

**2.5. Materials Cytotoxicity.** For materials cytotoxicity assay the primary bone marrow mesenchymal stromal cells (BM-MSCs) culture was established by placing 3 mL of bone marrow aspirate from the femora and tibiae of adult rats (180–200 g) in 25  $\text{cm}^2$  culture flasks in advMEM (Cat. No: 12491–015, Invitrogen) supplemented with 10% fetal bovine serum (FBS) (Cat. No: SH30070.03, HyClone). The protocol was approved by the Animal Ethics Committee of P.A. Hertenzen Moscow Oncology Research Institute. At confluence, the primary cells were trypsinized with 0.05% trypsin/EDTA solution (Cat. No: 25300062, Invitrogen) and passaged. Fluorescein diacetate (FDA) (Cat. No: F1303, Invitrogen) viability probe assay was used to estimate toxicity of the investigated materials. BM-MSCs were seeded at a density of  $1 \times 10^5$  cells/well of a 12 well plate in DMEM (Cat. No: 10566–032, Invitrogen) supplemented with 10% FBS and cultured during 18 h. Then 5 mg of each sample (OCP ceramic granules) was added per well. After 72 h, 0.5  $\mu\text{g}/\text{mL}$  of FDA was added to a well for 5 min. The fluorescence was measured by SpectraMax M5Multi-Mode Microplate Reader (Molecular Devices, USA).

**2.6. Animal Experiments.** All animal trials were performed in conformity with institutional guidelines in compliance with national laws and policies for Animal Care. The guidelines approved by the Animal Ethics Committee of National Hematology Research Centre and Central Scientific Research Institute of Dentistry and Maxillofacial Surgery.

**2.6.1. Subcutaneous and Kidney Capsule Implantation.** A total of 40 CBA/C57 Black C 12 weeks old mice were anesthetized by 4% isoflurane inhalation in sterile conditions. Three surgical procedures with the OCP ceramic granules were performed for each mouse: one subcutaneous (SC) beneath the dorsal skin between the scapulae with contralaterally placed 32  $\text{mm}^3$  of material and two under the both kidney capsules (KC) with placed 8  $\text{mm}^3$  of material. Five animals of each group were sacrificed with carbon dioxide and the specimens were retrieved at 2, 6, 12, and 18 weeks.

**2.6.2. Cranial and Distal Femoral Epiphysis Models.** 40 adult Wistar rats (12 weeks old, body weight 250–300 g of both sexes) were divided into two groups. For surgery, each rat was anesthetized by intraperitoneal injection of Zoletil 50 (Virbac S.A., France) with a dose of 0.2 mL/100 g of body weight. For the cranial model, an angular skin incision was performed on the skull. Bone defects 9 mm in diameter (using a pre-designed template) were created on the sagittal line of parietal region with a trephine under constant irrigation with NaCl 0.9%. In case of the femoral epiphysis model, an incision was made in the skin on the medial side of the thigh and the femoral quadriceps muscle was exposed. The muscle was sectioned longitudinally in its distal third and separated anterolaterally. After exposure of the distal end of the epiphysis of the right femur and peeling of the periosteum, a bone defect was created with a 3 mm hand-held surgical drill under irrigation of NaCl 0.9%. In the test group, OCP ceramic granules were inserted into the defect. In case of the cranial model, the bone defects were healed under a membrane made from alginate. In the control group, the bone defects were empty and healed under blood clots. The animals were sacrificed in 2, 4, 8, and 12 weeks.

**2.6.3. Histological Examination.** Grafts with surrounding tissues were dissected and fixated in 10% buffered formalin for 24 h. Each graft was sectioned in ten pieces through its midline and embedded in paraffin. Serial 5  $\mu\text{m}$  sections were deparaffinized, hydrated and stained with hematoxylin and eosin. Photomicrographs of internal sections of each sample were taken with light microscope (Leica DM LB,

Germany) and photographed (Sony, Japan). Computed-assisted measurements of the histological parameters were obtained using an automated image analysis system Image-Pro Plus (Media Cybernetics, USA).<sup>26</sup> For each graft at least 5 sections were examined, in each section at least 25 fields of vision were analyzed. The region of interest was taken at 100 $\times$  magnification and resolution of 2500  $\times$  1200 pixels.

**2.6.4. Immunohistochemistry.** Explanted from sacrificed mice graft materials were rinsed in ice-cold PBS, fixed for 24 h in 4% formaldehyde and placed in 70% EtOH until embedded in paraffin. The histological section (5  $\mu\text{m}$ ) was deparaffinized in *o*-xylol twice for 5 min and then three times for 5 min in 96% EtOH before the osteocalcin or CD34 IHC-staining. Antigen retrieval was achieved by heating the sections at  $95^{\circ}\text{C}$  in target retrieval solution (pH 6.0) (Cat. No: S1699, Dako) for 40 min. The activity of endogenous peroxidase was inhibited by 10 min exposure to 3%  $\text{H}_2\text{O}_2$  at room temperature. For osteocalcin detection the sections were incubated with primary mouse antihuman osteocalcin antibodies (Cat. No: MAB1419, R&D Systems) using Animal research kit (Cat. No: K3954, Dako), according to manufacturer's instructions and incubated with substrate-chromogen solution (Cat. No: DAB+, Dako). Sections were counterstained with Mayer's hematoxylin and mounted with Dako Glycergel Mounting Medium (Cat. No: C0563, Dako). Quantitative analysis for the intensity of immunohistochemistry dyeing was calculated by using ImageJ software by measuring the specific color intensity.<sup>27</sup> For each graft at least 5 sections were examined, in each section at least 25 fields of vision were analyzed.

**2.7. Clinical Cases.** The local clinical trial and the protocol for human tissue collection used in this study were approved by the State Research Centre Burnasyan Federal Medical Biophysical Centre of the FMBA of Russia. Written informed consents were obtained for each patient and were approved by State Research Centre Burnasyan Federal Medical Biophysical Centre of the FMBA of Russia. The study was aimed to evaluate safety and efficacy of the OCP granular material in the treatment of patients with different etiology bone defects and atrophy of jaws. All patients underwent clinical examination with assessment of general status, blood test, urine analysis, computed tomography (CT) (New Tom 3G, Italy) and checkup of the affected area before and after surgery. CT was performed to estimate baseline conditions of jaws defect or atrophy zones with measurement of their sizes and average density. A standard tool was used for definition of ROI (region of interest) average density and measurements of the target area on each section (1 mm step) were taken. 4–6 months after surgery bone biopsies for subsequent histological analysis (see section 2.6.3) were obtained during dental implantation.

**2.8. Statistical Analysis.** Results were expressed as the mean  $\pm$  standard deviation (SD). All experiments were performed with at least three individual replicates. Statistical analysis was performed by One-Way ANOVA and paired Student's *t* test (GraphPad Prism 5.0, GraphPad Software).<sup>28</sup> A *p*-value of less than 0.05 was considered statistically significant.

### 3. RESULTS AND DISCUSSION

There is a long-felt need of guidelines for scaffold design. It is well-known that the materials for bone tissue engineering should be with defined pore size three-dimensional structure, controlled interconnectivity, surface area and etc. The use of OCP granules and its efficacy in bone formation have been established by the previous studies.<sup>12,13,17–20</sup> However, all of the studies mentioned above were carried out with OCP granules that were prepared by lightly grinding the pressed dried OCP powders. The resulting materials were represented as dense agglomerates of irregular shape. In our study, we used a relatively simple processing route based on preparation of CC ceramics with designed and controlled microstructure through high-temperature treatment followed by a biphasic material process. Granules as the most appropriate formulation were used as a model.

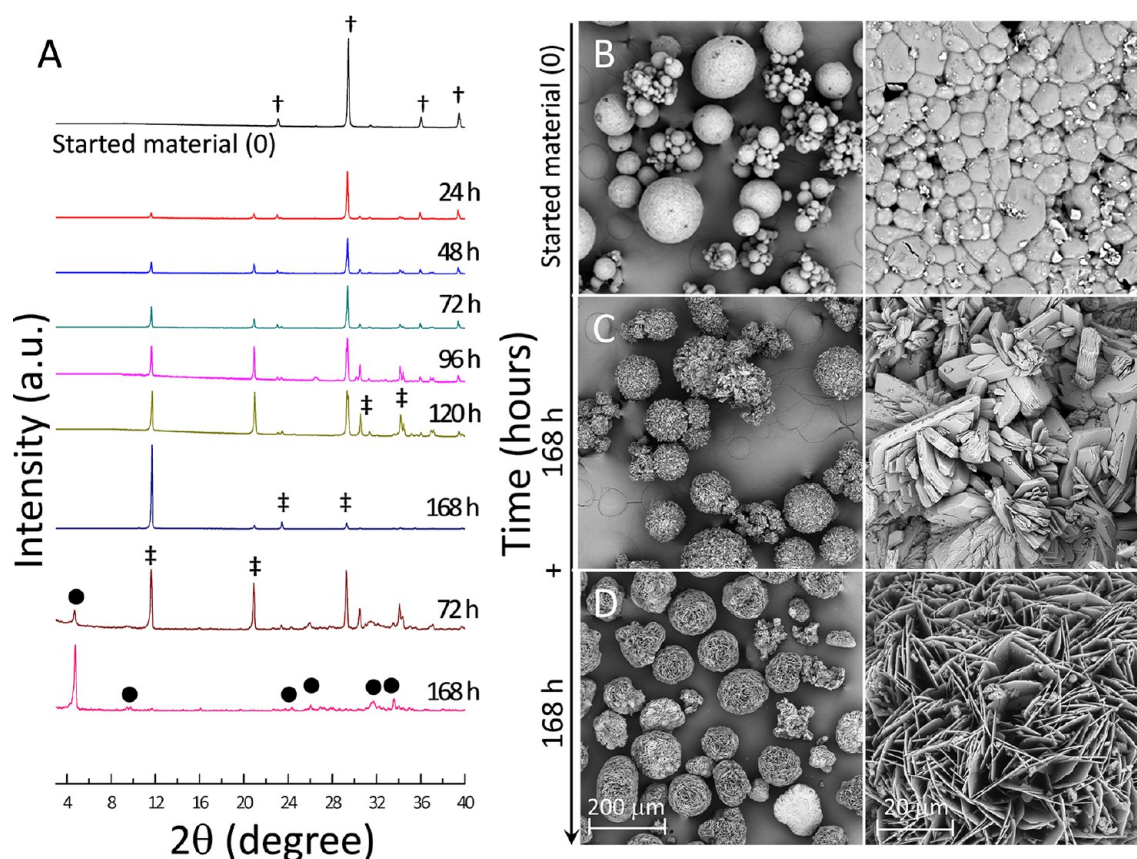


**Figure 1.** (A) XRD chart of the transformation of CC to OCP ceramic granules soaked in calcium nitrate solution during 168 h and in sodium acetate during 168 h. SEM photomicrographs of (B) CC (initial material), (C) DCPD (after soaking in calcium nitrate solution at 168 h) and (D) OCP (after soaking in sodium acetate at 168 h) ceramic granules.

At first, the calcium carbonate ceramics were transformed into dicalcium phosphate dihydrate (DCPD) ( $\text{CaHPO}_4 \cdot 2\text{H}_2\text{O}$ , Brushite). The process was completed after soaking in calcium nitrate solution during 168 h (Figure 1A). Scanning electron photomicrographs of both CC and DCPD ceramic granules are shown in Figure 1B, C. Particle size of the parent CC was about 5–10  $\mu\text{m}$  (Figure 1B). The DCPD crystals had a flowerlike morphology (i.e., morphology outside the common flat-plate type was observed). The width of the DCPD plates ranged from 1 to 25  $\mu\text{m}$  and their thickness was over the range from a fraction of a micron to several microns (Figure 1C). The morphology of DCPD crystals obtained by Mandel et al.<sup>29</sup> on the transformation of DCPD powders at 36.5 °C in Dulbecco's Modified Eagle Medium solutions was quite similar to those shown in Figure 1C. In this work, it was proposed that during synthesis of DCPD, calcium carbonate particles were chemically attacked by the acidic  $\text{H}_2\text{PO}_4^-$  ions in the solution, and a template synthesis-type reaction followed. The CC particles behaved as the template and the dumbbells of stacked DCPD water lilies gradually formed in the place of the original template. This process can be seen in Figure 2A, where the transformation from CC to DCPD was stopped after 24 h of soaking in the solution.

The obtained DCPD granules were transformed into OCP upon 168 h of soaking in sodium acetate, as shown by the XRD of Figure 1A. XRD of the OCP ceramic granules confirmed mainly OCP phase with following characteristic: (100) reflection at  $2\theta = 4.9^\circ$  (Figure 1A). However, the samples contained some small amount of unreacted DCPD upon 168 h

and new nucleated hydroxyapatite phase was detected after 168 h of soaking in sodium acetate. The high intensity and well-resolved diffraction peaks indicate on high crystallinity of OCP granules (Figure 1A). Subsequent DCPD hydrolysis enabled us to obtain both phase OCP or DCPD/OCP mixtures of controlled composition, depending on the process conditions (hydrolysis time). According to IR spectroscopy data, the spectrum of DCPD contained strong bands characteristic of this compound: ( $\nu_4$ ) at 575  $\text{cm}^{-1}$ , ( $\nu_1$ ) at 985  $\text{cm}^{-1}$ , and ( $\nu_3$ ) at 870, 1058, and 1126  $\text{cm}^{-1}$ ;  $\text{H}_2\text{O}$  at 661, 793, and 1650  $\text{cm}^{-1}$ ; and  $\text{OH}^-$  at 1226, 2386, 3159, and 3534  $\text{cm}^{-1}$ .<sup>30</sup> The IR spectra of the hydrolysis products (OCP) were significantly different from the spectrum of DCPD. The product of hydrolysis with 50 wt. percent OCP had a characteristic band of the group at 962  $\text{cm}^{-1}$  and bands assigned to phosphate groups: a doublet in the range 560–601  $\text{cm}^{-1}$  and bands in the range 860–962  $\text{cm}^{-1}$ .<sup>31</sup> The strong band assigned to  $\text{H}_2\text{O}$  vibrations at 1650  $\text{cm}^{-1}$  was shifted to 1638  $\text{cm}^{-1}$  and had a reduced intensity. Increasing the hydrolysis time produced a  $\text{OH}^-$  band at 3568  $\text{cm}^{-1}$ , characteristic of OCP. The spectra contained bands in the range 560–660  $\text{cm}^{-1}$  due to stretching vibrations of phosphate groups ( $\nu_4$ ). The IR spectra are presented in Figure 3.

OCP/DCPD composite samples contained platelike characteristic of DCPD (Figure 2B). The OCP crystals in the sample had the form of needles 2–5  $\mu\text{m}$  in length and 1–2  $\mu\text{m}$  in width, whose dimensions were similar to those of the parent DCPD platelets (Figure 1C). The SEM data are consistent with trends in the variation of the crystallite size estimated for the

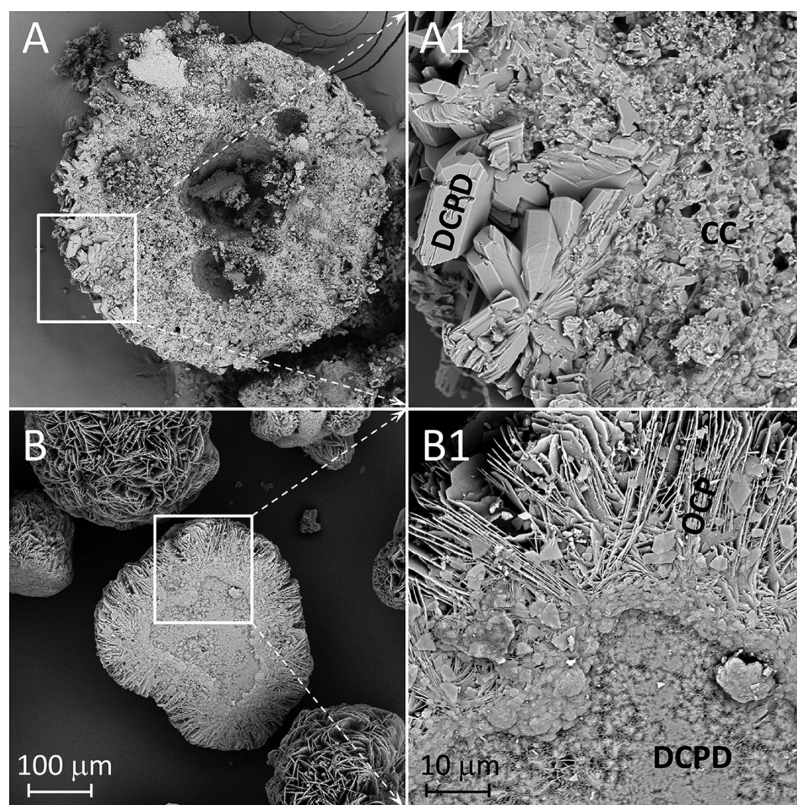


**Figure 2.** SEM photomicrographs of samples where the transformation from CC to OCP was stopped after (A) 24 and (B) 72 h of soaking in calcium nitrate solution and in sodium acetate, respectively. (A1, B1) Granule incision in the middle.

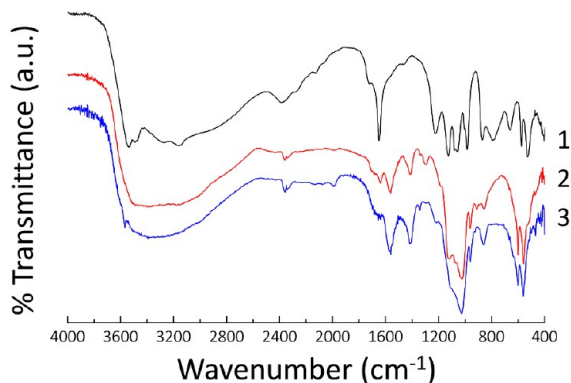


**Figure 3.** IR spectra of (1) DCPD, (2) OCP/DCPD, and (3) OCP products.

synthesized compounds: DCPD transformation into OCP was accompanied by a decrease in particle size of the DCPD (Figure 1C, D).

Final physicochemical characteristics of the biomaterial are presented in Table 1. Figure 1D shows scanning electron micrographs of OCP ceramic granules microstructure. The size was 0.1–20.0  $\mu\text{m}$ . They exhibited a lamellar morphology (Figure 1D) with a very large surface area (Table 1). These OCP granules were used for further experiments.

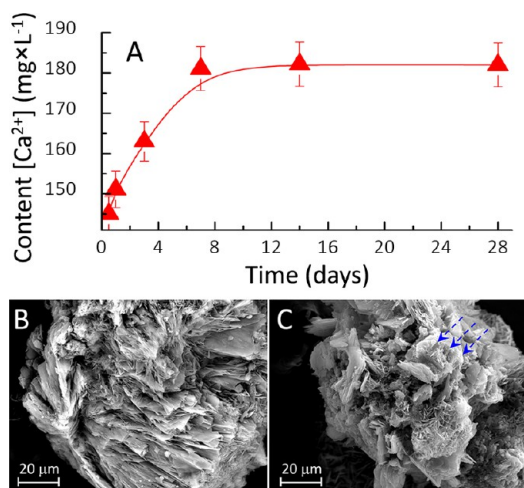
**Table 1.** Characteristics of the OCP Ceramic Granules

phase composition	diameter of granules ( $\mu\text{m}$ )	intergranular porosity (%)	overall porosity (%)	pore size ( $\mu\text{m}$ )	BET surface area ( $\text{m}^2/\text{g}$ )
octacalcium phosphate (OCP)	$500 \pm 100$	$\sim 32$	$\sim 61$	$\sim 0.1\text{--}20$	21.008

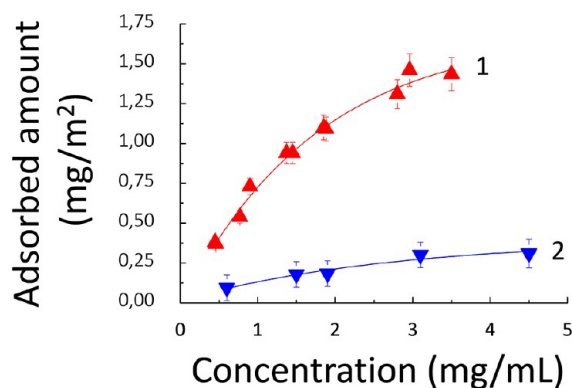
It is important to note here that the chemical transformation of CC into DCPD, followed by DCPD hydrolysis to OCP allowed to produce mainly phase pure OCP ceramic granules or calcium phosphate mixtures with variable CC/DCPD and DCPD/OCP ratios (Figure 1A). The ratio of these ceramics could be controlled by treating time. The concept of a biphasic material could be taken in account for engineering artificial bone grafts in future research.

Figure 4A shows the dissolution curve of the OCP ceramic granules as a function of time. The calcium content in the solution reaches a plateau at 14 days of the investigated period. This is due to the completion of the phase composition development with high contents of highly soluble constituents such as OCP and probably, saturation of the solution. According to SEM observation OCP ceramic granules were deformed completely and had the diameter 200–250  $\mu\text{m}$  after 28 days of the degradation test (Figure 4C). The morphology of OCP crystals was changed and the hydrolyzed apatite was observed (Figure 4C and Figure S1 in the Supporting Information). It is well-known that OCP is metastable phase with respect to HA; thus, OCP converted spontaneously to HA during the dissolution test.

Protein adsorption on biomaterials has significant importance in biomedical applications.<sup>32</sup> Figure 5 shows the adsorption isotherms calculated from the data obtained at 20 h. The plots are characterized by an initial slope indicating a



**Figure 4.** (A) Dissolution behavior of the OCP ceramic granules as a function of time. SEM photomicrographs of the OCP ceramic granules after solubility test ((B) 14 and (C) 28 days). Arrowheads represent the hydrolyzed apatite.



**Figure 5.** Isotherms of (1) BSA and (2) PL adsorbed onto OCP ceramic granules (equilibration time 20 h).

high affinity binding of the proteins for the OCP surface. The results indicated that adsorption strongly depended on the bulk concentration of the protein solutions; the adsorbed amount gradually increased with the protein solution concentration. The adsorption isotherms (Figure 5) indicated that BSA demonstrated the highest adsorption for increasing concentrations of solutions. After 20 h of incubation with solutions of 0.5 and 3.5 mg mL<sup>-1</sup> of BSA, adsorption onto OCP ceramic granules increased, respectively, to 0.37 and 1.45 mg m<sup>-2</sup>, whereas for PL this variation was around 0.08 and 0.32 mg m<sup>-2</sup>. The adsorption saturation yielded a plateau value corresponding to the maximum amount of BSA and PL surface uptake. The adsorption saturation value was about 1.45 mg m<sup>-2</sup> of BSA on OCP ceramic granules. This value was about two times higher than reported elsewhere,<sup>33</sup> with observed a BSA adsorption limit on hydroxyapatite in the range of 0.6 mg m<sup>-2</sup>. In case of PL, the adsorption saturation value was 0.3 mg m<sup>-2</sup>. Effect of the surface area of OCP ceramic granules on the ability of PL adsorption is shown in Table S1 in the Supporting Information. In general, the OCP ceramic granules were characterized by a high capacity to adsorption of these proteins with different degree that could affect the biological function of bone-forming cells during OCP implantation. In the review of Albrektsson and Johansson<sup>34</sup> the ability of OCP materials to

affect the biological function has been proposed that could partly be explained by the interaction with proteins during new bone formation.

We further studied cells proliferation as an indicator of materials toxicity. Seven days of coculture of BM-MSCs and OCP ceramic granules have shown the normal rate of proliferation. Therefore, OCP ceramic granules could be used for in vivo experiments. The cell growth and cytotoxicity analysis of BM-MSCs are presented in Figure's S2 and S3 of the Supporting Information.

A wide variety of ectopic locations have been used for experimentation, including subcutaneous, intramuscular, and kidney capsule transplantation. Subcutaneous implantation is the simplest method. However, the most pertinent concern is the relative paucity of bone formation in comparison to other models.<sup>35</sup> Therefore, we used two models for the comparison. The kidney capsule method is less widely used and is more technically challenging. But it allows for supraphysiologic blood and nutrient resource, promoting robust bone growth.<sup>35</sup> Subcutaneous and kidney capsule implantations of OCP ceramic granules in mice for 2–18 weeks showed no evidence of obvious inflammation response (Figure 6A). Histological

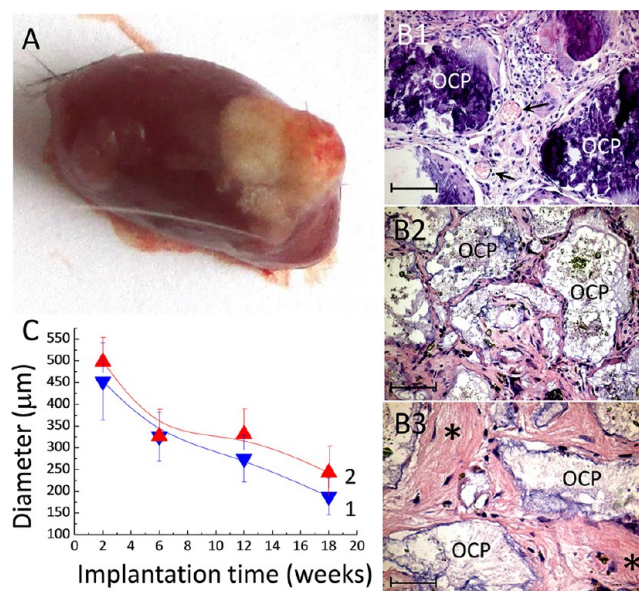


**Figure 6.** (A) Photomicrograph of the kidney capsule implantations of OCP ceramic granules in mice for 2 weeks. Histological examination of OCP ceramic granules for (B1) 2, (B2) 6, and (B3) 18 weeks after implantation (hematoxylin and eosin staining). Arrowheads represent blood vessels. Asterisk = connective tissue like layer. Bars = 200 μm. (C) The degradation profile vs the diameter of the OCP ceramic granules as a function of time (1, SC; 2, KC).

examination 2 weeks after implantation showed appearance of newly formed vessels surrounding the OCP ceramic granules (Figure 6B1). Multinucleate giant cells were in contact with OCP beads residuals at 4 and 6 weeks (Figure 6B2). After a prolonged time (12–18 weeks), degradation of OCP ceramic granules was also demonstrated, as evidenced by an increase in the connective tissue like layer (Figure 6B3). The data confirmed the ability of OCP ceramic granules to resorb in vivo. Figure 6C shows the degradation profile vs the diameter of the OCP ceramic granules as a function of time. The OCP ceramic granules that were implanted SC beneath the dorsal

skin between the scapulae and under KC were positively stained for osteocalcin in both cases (Figure 7A, B). The

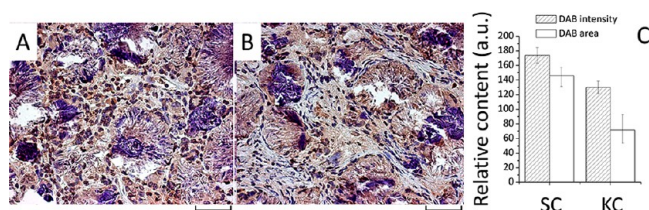


**Figure 7.** Photomicrographs of the immuno-staining for osteocalcin on 2 weeks: (A) SC, (B) KC. Bar = 500  $\mu$ m. (C) The gene expression profiles in OCP granules. Data are represented as mean  $\pm$  SE.

presence of the bone building protein synthesized exclusively by osteoblasts and odontoblasts was confirmed. Expressions of osteocalcin were stronger in the case of SC implantation (Figure 7C). These results suggest that the OCP ceramic granules have the ability to form bone tissue in heterotopic models.

The OCP ceramic granules were implanted into the cranial and distal femoral epiphysis to determine whether bone regeneration could be activated through tissue–material interactions in the early stage. In the case of the cranial model (Figure 8A), the control defects (i.e., empty drill defects) were interspaced by fibro-connective tissues with very small amount of new bone close to the boundary area after 4 and 12 weeks of implantation (Figure 8B, C). Histological sections of the implanted OCP ceramic granules demonstrated different results (Figure 8D). Most of the OCP ceramic

granules were attacked by bonelike cells (Figure 8D1) and tended to be encapsulated with the newly formed bone in 4 weeks (Figure 8D2). After 12 weeks of implantation, bone apposition occurred directly on the surfaces of these granules without formation of fibrous tissue. Bone marrow was also formed within the bone regenerate (Figure 8F). Thus, the OCP ceramic granules simulated bone formation more significantly than the control group throughout the implantation periods. The percentage of newly formed bone in the defect was assessed by histomorphometry. The data are presented in Table 2. The rate of bone formation was differed depending on the

**Table 2.** Percentage of Newly Formed Bone (%)<sup>a</sup>

group	4 weeks		12 weeks	
	boundary area	central area	boundary area	central area
control	12 $\pm$ 4.8		18 $\pm$ 6.0	
OCP ceramic granules	37 $\pm$ 10 <sup>b</sup>		49 $\pm$ 15 <sup>b</sup>	28 $\pm$ 7 <sup>b</sup>

<sup>a</sup>Each value is expressed as mean  $\pm$  SD. <sup>b</sup>Difference compared to the control group in the same period are statistically significant ( $p < 0.05$ ).

site of the defect. The degradation of OCP ceramic granules observed mainly at 12 weeks of implantation (see Table S2 in the Supporting Information).

In the case of femoral epiphysis model, a small amount of newly formed bone and bone marrow were observed on 4 weeks (Figure 9A1) in the control defects (i.e., empty drill defects). After 8 weeks, there were no signs of earlier formed trabecular bone in the defect and the defect mainly remodeled

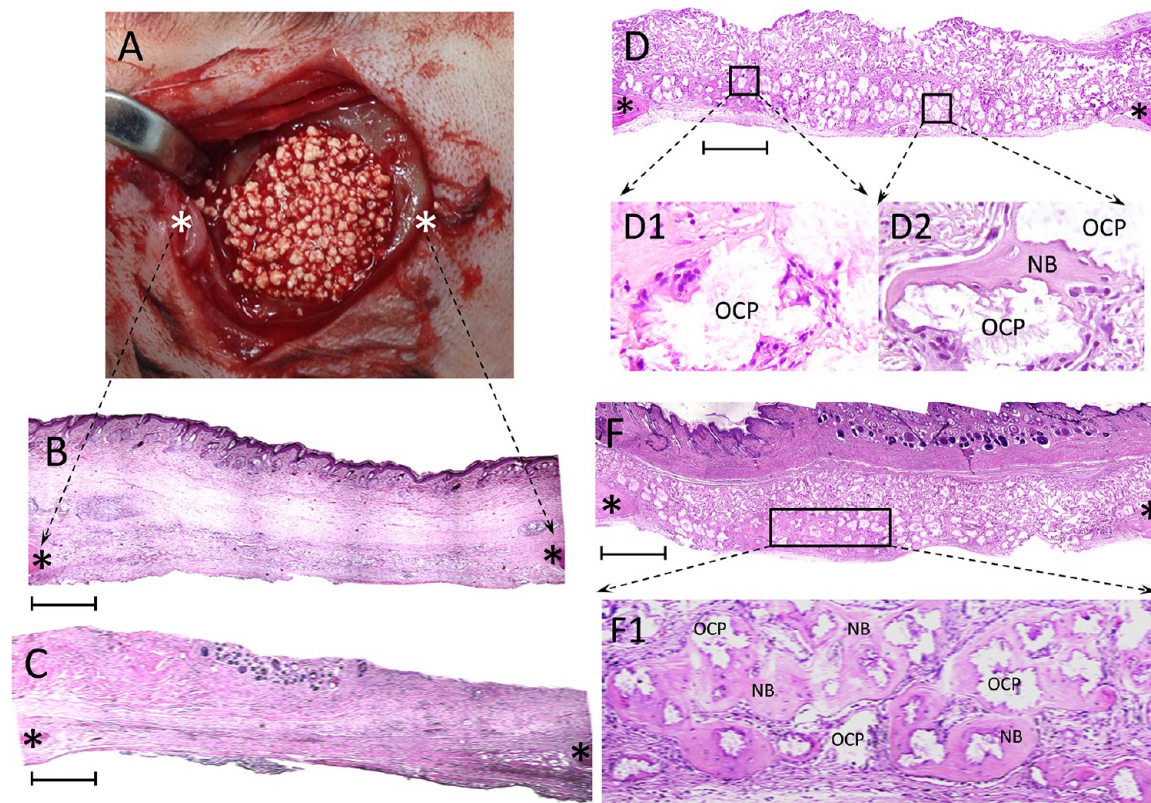


**Figure 8.** (A) Photomicrograph of the cranial defect produced. Photomicrographs of decalcified histological sections stained with (B, C) hematoxylin and eosin for control and (D, F) OCP ceramic granules for 4 and 12 weeks implantation, respectively. (B–F) Bar = 1 mm. (D1, D2, F1) Zoom of the region of interest. NB, newly formed bone.

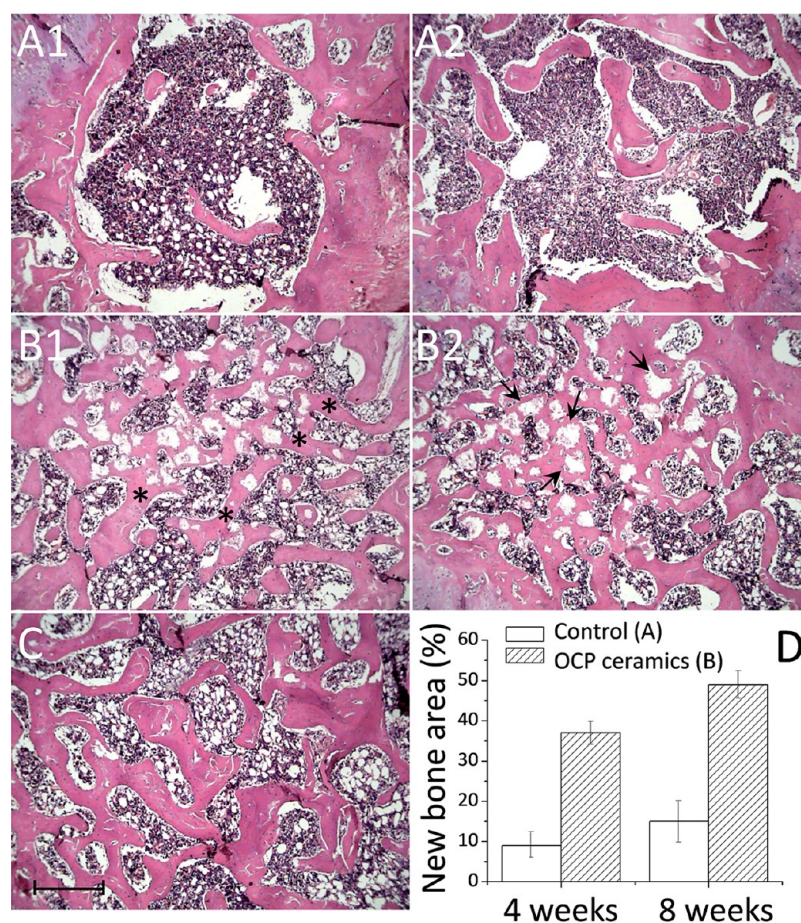


**Figure 9.** Photomicrographs of decalcified histological sections stained with (A1, A2) hematoxylin and eosin for control and (B1, B2) OCP ceramic granules for 4 and 8 weeks implantation, respectively. (C) Histological section of native bone. (A–C) Bar = 1 mm. (D) The percentage of newly formed bone was for the control defects and for the OCP groups after 4 and 8 weeks of implantation. Arrowheads represent OCP ceramic granules. Asterisk = newly formed bone.

and partly replaced by fibrous tissue (Figure 9A2). In the OCP group, bone formation was observed already after 4 weeks of the experiment (Figure 9B1). After 8 weeks, newly formed bone in the defect had quasi trabecular structure (Figure 9B2). These data indicate that OCP material enhanced regeneration of trabecular bone with architecture equivalent to normal bone tissue (Figure 9C). Partially degraded OCP ceramic granules were included in the bone regenerate. Degradation of OCP ceramic granules in this model has already been observed at 4 weeks of implantation (see Table S2 in the Supporting Information). The percentage of new bone was  $9.1 \pm 5.3$  and  $13.3 \pm 7.5$  for the control defects, and  $34.2 \pm 6.9$  and  $49 \pm 8.2$  for the OCP groups after 4 and 8 weeks of implantation, respectively (Figure 9D). Statistical analysis revealed significant difference ( $p < 0.05$ ) between the control and the OCP groups. The kinetic feature of bone formation in the OCP group is presented in Figure S4 of the Supporting Information. After 2 weeks, new bone was already formed around the surface of OCP ceramic granules, which is common for synthetic materials (see Figure S4A in the Supporting Information). However, a more detailed look at the histological data revealed that a connective tissue-like layer in the form of bridges started to grow between OCP ceramic granules at this period (see Figure S4A1 in the Supporting Information). Eventually this tissue was transformed into newly formed bone with trabecular structure (Figure S4B, C in the Supporting Information). It is

interesting to note that the bridges grew in the direction of the shortest distance between the ceramic beads. We made a comparison of OCP granules with well-known commercial TCP based materials as it is shown in Figure S5 in the Supporting Information. The kinetics of bone formation was quite different from the OCP group. The newly formed bone was presented only around TCP particles.

It is well-known that synthetic bone graft substitutes are osteoconductive. This term means that bone grows on a surface of a substitute. In other words, it has been suggested that osteoconduction is the process by which bone is directed to conform to a material's surface.<sup>34</sup> Ideally a material must be osteoinductive, i.e., undifferentiated and pluripotent cells are somehow stimulated to develop into the bone-forming cell lineage and a bone graft would induce new bone formation in an intraosseous defect.<sup>34,36,37</sup> OCP ceramic granules reported in this study at least possessed enhanced capacity of new bone formation, which was close to normal bone tissue and some ability to form bone tissue in heterotopic models. These data suggested that the developed material did not satisfy completely the definitions of osteoconductivity and osteoinductivity. To overcome this obscurity, we proposed to introduce a new definition "osteotransductivity". By this term, we mean that an osteotransductive material is the one that converts a stimulus from body environment to form new bone tissue. The high potential of OCP ceramic granules raises questions about the



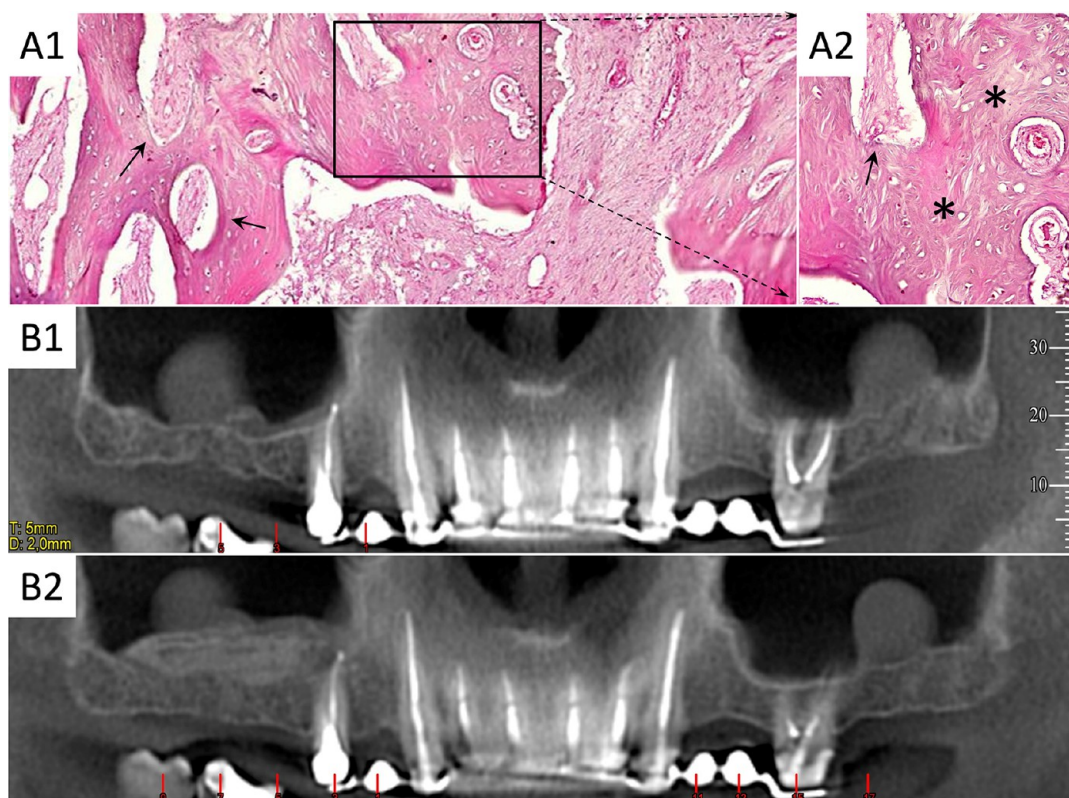


**Figure 10.** Bone biopsy after OCP ceramic granules implantation. Clinical case I: (A1) column of bone tissue separated in several areas by fibrous tissue; (A2) region of woven bone regenerate. Arrowheads represent OCP ceramic granules. Asterisk = newly formed bone. Staining: hematoxylin and eosin. Magnification: A1,  $\times 100$ ; A2,  $\times 200$ . Clinical case II: maxilla (B1) before and (B2) after operation. Multispiral computer tomography, panoramic reconstruction.

nature of such properties (the chemical composition or microstructural properties) and cellular and molecular mechanisms behind it. Our working hypothesis is that OCP ceramic granules have such potential because of the phase composition as well as to their crystal morphology and the specific surface area. It has been proposed that OCP could play an important role in apatite crystal development as a precursor of biological apatite.<sup>38</sup> In contrast to that, the lamellar crystals OCP ceramic granules with enlarged surface have high protein adsorption capacity that can affect the biological function of bone-forming cells during implantation. However, there are a number of questions that remain unsolved and could be discovered in the future research.

In the frame of this manuscript, we sought to describe preliminary results of the local clinical trial on two patients.

**Clinical Case I.** Female (37 years old) was included into the study with histologically verified diagnosis “fibrous dysplasia at the frontal part of mandible”. The disease was asymptomatic and detected accidentally during radiographic examination. At the level of 3.1–4.2 teeth’s light prominence of free mucosa was observed, that corresponded to bone destruction region with clear contours, irregular shape and alternating areas of low and high density detected by CT scan. Also, the small defects of vestibular and lingual cortical plates were identified.

In accordance with diagnosis and fibrous dysplasia volume, excochleation of pathological tissues with simultaneous bone grafting were indicated for clinical case 1 after endodontic preparation (canal filling) of 3.3–4.3 teeth. Under endotracheal narcosis and local anesthesia (Ultracain DS with 1:200000 epinephrine hydrochloride) incision was made on the line of

free mucosa at the level of 3.4–4.4 teeth, mucoperio steal flap was peeled with exposure of the bone surface. The defect of vestibular cortical plate was widened with removal of pathological fibrous tissue and processing of bone defects walls up to the intact bone by milling dental bur. Root apices of 3.3–4.3 teeth were resected. The defect was filled with about 5 g of OCP ceramic granules. Postoperative wound was closed with a continuous suture (Caprolon4/0).

There were no complications in postoperative period. According to the control CT scan performed 4.5 months after surgery, the bone defects at the frontal part of the mandible were substituted with new bone of heterogeneous structure, the average density was  $691.9 \pm 123.6$  HU that matched intact cancellous bone density. Trepan-biopsy was performed on the same period as CT-scan and was presented as a column of hard tissue, not less than 60% of which consisted of newly formed bone (Figure 10A). Woven bone tissue of the regenerate was characterized by tendency to remodeling in a lamellar bone. OCP ceramic granules were only detected in some of bone trabeculae. Newly formed vessels could be seen in some of the remaining granules that appeared like osteon formation.

**Clinical Case II.** Male (32 years old) with atrophy of maxilla alveolar process with partial secondary edentia of upper and lower jaws. According to CT scan, thickness of alveolar ridge in projection of absent 1.6–1.8 teeth was 4.4–5.8 mm. (Figure 10 B1).

This patient underwent sinus floor augmentation. Under local anesthesia (Ultracain DS with 1:200000 epinephrine hydrochloride) through the formed “window” in the lateral wall

of the right sinus, the Schneider membrane was carefully lifted, and about 3 g of OCP ceramic granules were placed into the newly formed space between sinus floor and a collagen membrane placed under the tunica mucosa to separate it from OCP ceramic granules. The fragment of sinus wall was placed back to close the window, postoperative wound sutured by Caprolon 4/0.

Postoperative adverse events were not observed, the wound healed with no signs of acute inflammation. According to the CT scan 4.5 months after sinus lifting with implantation of OCP ceramic granules, the thickness of maxilla alveolar process reached 11.3–17.8 mm due to regeneration that was formed in the area of tissue-engineered material implantation. The regenerate was completely integrated with underlying bone, characterized by relatively homogeneous structure, and the average density  $821.3 \pm 74.1$  HU, which was slightly higher than the density of intact cancellous bone (Figure 10B2).

Analyzing the results of the two clinical cases, we can postulate that 4.5 months after surgery the majority of OCP granules were not seen in newly formed tissue by CT-scan. According to our data, the initial density of OCP granules is measured in average 1800 HU, whereas the density of regenerates were  $691.9 \pm 123.6$  HU and  $821.3 \pm 74.1$  HU in clinical cases 1 and 2, respectively, at the last time point. So, the density of newly formed tissue was slightly higher than native cancellous bone of the maxilla' alveolar process has but significantly less than it is typical for OCP ceramic granules. Relative homogeneity of regenerates in all cases and the absence of "contrast" particles therein proved resorption of the granules and their substitution by regenerate. Histological analysis confirmed the CT-scan results. We found only OCP ceramic granules "footprints" in the newly formed trabecular bone, retained obviously due to vessels growth followed by connective tissue. These data taken together suggest that at least a large part of the OCP ceramic granules was resorbed and replaced by bone regenerate after 4.5 months follow-up that provided such a positive outcome. Complementary, in order to meet other requirements for successful bone repair, such as mechanical and handling properties the developed route could be applied to produce bulk materials. For instance, we were able to design structure by chemical transformation of ceramic into OCP material obtained by traditional replicate technique (see Figure S6A in the Supporting Information), 3D printing methodology platform (see Figure S6B in the Supporting Information)<sup>39</sup> and composite materials based on OCP and polymers (see Figure S6C in the Supporting Information).

## CONCLUSIONS

We developed a simple method to produce OCP ceramic granules with a specifically designed microstructure and phase compositions that depended on the preparation route. Using this method, we have obtained the flat plate OCP crystals with enlarged surface area, controlled resorption rate and high capacity to proteins adsorption. Immunohistochemical analysis showed that OCP ceramic granules stimulated osteocalcin synthesis in subcutaneous and kidney capsule models. Qualitative histology proved biocompatibility, osteoconduction, osteotransduction, and favorable resorption, that was realized mainly through a cell-mediated mechanism. The results indicate that OCP ceramic granules have osteogenic features of interest and are able to simulate lamellar bone formation 2 months after in vivo implantation. 4–5 months after implantation of OCP materials, computed tomography and histological examinations

of patient's biopsies of the treated defect revealed the newly formed bone. Therefore, the developed OCP material can be recommended as a synthetic alternative to others bone substitutes or as a scaffold material of "activated" grafts in regenerative medicine.

## ASSOCIATED CONTENT

### Supporting Information

XRD patterns of OCP ceramic granules after solubility test, effect of the surface area of OCP ceramic granules on the ability of PL adsorption, cell growth and cytotoxicity analysis of BM-MSCs immobilized on OCP ceramic granules, OCP ceramic granules induced osteogenic differentiation of BM-MSCs, dissolution behavior of the OCP ceramic granules as a function of time vs diameter, photomicrographs of decalcified histological sections stained with hematoxylin and eosin for Ceracor (Curasan AG, Germany) for 4 and 8 weeks implantation and SEM photomicrographs of the obtained OCP-based materials by traditional replicate technique, 3D printing methodology platform and composite spongy material based on OCP ceramic granules and fibrinogen. This material is available free of charge via the Internet at <http://pubs.acs.org/>.

## AUTHOR INFORMATION

### Corresponding Author

\*E-mail: [komlev@mail.ru](mailto:komlev@mail.ru). Telephone/Fax: +7 495-437-9740.

### Author Contributions

The manuscript was written through contributions of all authors. All authors have given approval to the final version of the manuscript.

### Notes

The authors declare no competing financial interest.

## ACKNOWLEDGMENTS

This work was supported by the Russian Foundation for Basic Research (Grants 12-03-33074, 12-03-00704, 13-04-12025) and the Russian Foundation for Assistance to Small Innovative Enterprises in Science and Technology (Contract 12184 p/23097).

## REFERENCES

- (1) Kolk, A.; Handschel, J.; Drescher, W.; Rothamel, D.; Kloss, F.; Blessmann, M.; Heiland, M.; Wolff, K. D.; Smeets, R. Current Trends and Future Perspectives of Bone Substitute Materials - from Space Holders to Innovative Biomaterials. *J. Craniomaxillofac. Surg.* **2012**, *40*, 706–718.
- (2) Dorozhkin, S. V. Calcium Orthophosphates in Nature Biology and Medicine. *Materials* **2009**, *2*, 399–498.
- (3) Daculsi, G. Biphasic Calcium Phosphate Concept Applied to Artificial Bone, Implant Coating and Injectable Bone Substitute. *Biomaterials* **1998**, *19*, 1473–1478.
- (4) Lobo, S. E.; Arinze, L. T. Biphasic Calcium Phosphate Ceramics for Bone Regeneration and Tissue Engineering Applications. *Materials* **2010**, *3*, 815–826.
- (5) Suba, Z.; Takács, D.; Matusovits, D.; Barabás, J.; Fazekas, A.; Szabó, G. Maxillary Sinus Floor Grafting with b-Tricalcium Phosphate in Humans: Density and Microarchitecture of the Newly Formed Bone. *Clin. Oral Implants Res.* **2006**, *17*, 102–108.
- (6) Horowitz, R. A.; Mazor, Z.; Foitzik, C.; Prasad, H.; Rohrer, M.; Palti, A. b-tricalcium Phosphate as Bone Substitute Material: Properties and Clinical Applications. *J. Osseointegr.* **2010**, *2*, 61–68.
- (7) Stavropoulos, A.; Windisch, P.; Szendrői-Kiss, D.; Peter, R.; Gera, I.; Sculean, A. Clinical and Histologic Evaluation of Granular Beta-tricalcium Phosphate for the Treatment of Human Intra-bony

Periodontal Defects: a Report on Five Cases. *J. Periodontol.* **2010**, *81*, 325–334.

(8) Suzuki, O.; Kamakura, S.; Katagiri, T. Surface Chemistry and Biological Responses to Synthetic Octacalcium Phosphate. *J. Biomed. Mater. Res., Part B* **2006**, *77*, 201–212.

(9) Shelton, R. M.; Liu, Y.; Cooper, P. R.; Gbureck, U.; German, M. J.; Barralet, J. E. Bone Marrow Cell Gene Expression and Tissue Construct Assembly using Octacalcium Phosphate Microscaffolds. *Biomaterials* **2006**, *27*, 2874–2881.

(10) Liu, Y.; Cooper, P. R.; Barralet, J. E.; Shelton, R. M. Influence of Calcium Phosphate Crystal Assemblies on the Proliferation and Osteogenic Gene Expression of Rat Bone Marrow Stromal Cells. *Biomaterials* **2007**, *28*, 1393–1403.

(11) Barinov, S. M.; Komlev, V. S. Osteoinductive Ceramic Materials for Bone Tissue Restoration: Octacalcium Phosphate (Review). *Inorg. Mater. Appl. Res.* **2010**, *1*, 175–181.

(12) Suzuki, O.; Nakamura, M.; Miyasaka, Y.; Kagayama, M.; Sakurai, M. Bone Formation on Synthetic Precursors of Hydroxyapatite. *Tohoku J. Exp. Med.* **1991**, *164*, 37–50.

(13) Suzuki, O.; Nakamura, M.; Miyasaka, Y.; Kagayama, M.; Sakurai, M. Maclura Pomifera Agglutinin-Binding Glycoconjugates on Converted Apatite from Synthetic Octacalcium Phosphate Implanted into Subperiosteal Region of Mouse Calvaria. *Bone Miner.* **1993**, *20*, 151–166.

(14) Handa, T.; Anada, T.; Honda, Y.; Yamazaki, H.; Kobayashi, K.; Kanda, N.; Kamakura, S.; Echigo, S.; Suzuki, O. The Effect of an Octacalcium Phosphate Co-Precipitated Gelatin Composite on the Repair of Critical-Sized Rat Calvarial Defects. *Acta Biomater.* **2012**, *8*, 1190–1200.

(15) Barrere, F.; van der Valk, C. M.; Dalmeijer, R. A.; van Blitterswijk, C. A.; de Groot, K.; Layrolle, P. *In Vitro* and *In Vivo* Degradation of Biomimetic Octacalcium Phosphate and Carbonate Apatite Coatings on Titanium Implants. *J. Biomed. Mater. Res., Part A* **2003**, *64*, 378–387.

(16) Habibovic, P.; van der Valk, C. M.; van Blitterswijk, C. A.; de Groot, K.; Meijer, G. Influence of Octacalcium Phosphate Coating on Osteoinductive Properties of Biomaterials. *J. Mater. Sci.: Mater. Med.* **2004**, *15*, 373–380.

(17) Imaizumi, H.; Sakurai, M.; Kashimoto, O.; Kikawa, T.; Suzuki, O. Comparative Study on Osteoconductivity by Synthetic Octacalcium Phosphate and Sintered Hydroxyapatite in Rabbit Bone Marrow. *Calcif. Tissue Int.* **2006**, *78*, 45–54.

(18) Miyatake, N.; Kishimoto, K. N.; Anada, T.; Imaizumi, H.; Itoi, E.; Suzuki, O. Effect of Partial Hydrolysis of Octacalcium Phosphate on Its Osteoconductive Characteristics. *Biomaterials* **2009**, *30*, 1005–1014.

(19) Murakami, Y.; Honda, Y.; Anada, T.; Shimauchi, H.; Suzuki, O. Comparative Study on Bone Regeneration by Synthetic Octacalcium Phosphate with Various Granule Sizes. *Acta Biomater.* **2010**, *6*, 1542–1548.

(20) Kawai, T.; Echigo, S.; Matsui, K.; Tanuma, Y.; Takahashi, T.; Suzuki, O.; Kamakura, S. First Clinical Application of Octacalcium Phosphate Collagen Composite in Human Bone Defect. *Tissue Eng., Part A* **2014**, *20*, 1336–1341.

(21) Komlev, V. S.; Barinov, S. M.; Koplík, E. V. A Method to Fabricate Porous Spherical Hydroxyapatite Granules Intended for Time-Controlled Drug Release. *Biomaterials* **2002**, *23*, 3449–3454.

(22) Smirnov, V. V.; Bakunova, N. V.; Barinov, S. M.; Gol'dberg, M. A.; Kutsev, S. V.; Shvorneva, L. I. Effect of Ripening Time on the Sintering of CaCO<sub>3</sub> Powders and the Properties of the Resultant Ceramics. *Inorg. Mater.* **2012**, *48*, 544–548.

(23) Tas, A. C. Granules of Brushite and Octacalcium Phosphate from Marble. *J. Am. Ceram. Soc.* **2011**, *94*, 3722–3726.

(24) Shanskii, Ya.D.; Sergeeva, N. S.; Sviridova, I. K.; Kirakozov, M. S.; Kirsanova, V. A.; Akhmedova, S. A.; Antokhin, A. I.; Chissov, V. I. Human Platelet Lysate as a Promising Growth-Stimulating Additive for Culturing of Stem Cells and Other Cell Types. *Bull. Exp. Biol. Med.* **2013**, *156*, 146–151.

(25) Lowry, O. H.; Rosebrough, N. J.; Farr, A. L.; Randall, R. J. Protein Measurement with the Folin Phenol Reagent. *J. Biol. Chem.* **1951**, *193*, 265–275.

(26) Media Cybernetics - Image Analysis Software. <http://www.mediacy.com/> (accessed August 21, 2014).

(27) RSB Home Page. <http://rsbweb.nih.gov/> (accessed August 21, 2014).

(28) Home - graphpad.com. <http://www.graphpad.com/> (accessed August 21, 2014).

(29) Mandel, S.; Tas, A. C. Brushite (CaHPO<sub>4</sub>·2H<sub>2</sub>O) to Octacalcium Phosphate (Ca<sub>8</sub>(HPO<sub>4</sub>)<sub>2</sub>(PO<sub>4</sub>)<sub>4</sub>·5H<sub>2</sub>O) Transformation in DMEM Solutions at 36.5 °C. *Mater. Sci. Eng., C* **2010**, *30*, 245–254.

(30) Rau, J. V.; Fosca, M.; Komlev, V. S.; Fadeeva, I. V.; Albertini, V. R.; Barinov, S. M. In Situ Time Resolved Studies of Octacalcium Phosphate and Dicalcium Phosphate Dihydrate in Simulated Body Fluid: Cooperative Interactions and Nanoapatite Crystal Growth. *Cryst. Growth Des.* **2010**, *10*, 3824–3834.

(31) Rokidi, S.; Combes, C.; Koutsoukos, P. G. The Calcium Phosphate–Calcium Carbonate System: Growth of Octacalcium Phosphate on Calcium Carbonates. *Cryst. Growth Des.* **2011**, *11*, 1683–1688.

(32) Alves, C. M.; Reis, R. L.; Hunt, J. A. The Competitive Adsorption of Human Proteins onto Natural-Based Biomaterials. *J. R. Soc. Interface* **2010**, *7*, 1367–1377.

(33) Kandori, K.; Fudo, A.; Ishikawa, T. Adsorption of Myoglobin onto Various Synthetic Hydroxyapatite Particles. *Phys. Chem. Chem. Phys.* **2000**, *2*, 2015–2020.

(34) Albrektsson, T.; Johansson, C. Osteoinduction, Osteoconduction and Osseointegration. *Eur. Spine J.* **2001**, *10*, S96–S101.

(35) Scott, M. A.; Levi, B.; Askarinam, A.; Nguyen, A.; Rackohn, T.; Ting, K.; Soo, C.; James, A. W. Brief Review of Models of Ectopic Bone Formation. *Stem Cells Dev.* **2012**, *21*, 655–667.

(36) Barradas, A. M. C.; Yuan, H.; van Blitterswijk, C. A.; Habibovic, P. Osteoinductive Biomaterials: Current Knowledge of Properties, Experimental Models and Biological Mechanisms. *Eur. Cells Mater.* **2011**, *21*, 407–429.

(37) Yuan, H.; Fernandes, H.; Habibovic, P.; de Boer, J.; Barradas, A. M.; de Ruiter, A.; Walsh, W. R.; van Blitterswijk, C. A.; de Bruijn, J. D. Osteoinductive Ceramics as a Synthetic Alternative to Autologous Bone Grafting. *Proc. Natl. Acad. Sci. U.S.A.* **2010**, *107*, 13614–13619.

(38) Suzuki, O. Biological Role of Synthetic Octacalcium Phosphate in Bone Formation and Mineralization. *J. Oral Biosci.* **2010**, *52*, 6–14.

(39) Popov, V. K.; Komlev, V. S.; Chichkov, B. N. Calcium Phosphate Blossom for Bone Tissue Engineering 3D Printing Scaffolds. *Mater. Today* **2014**, *17*, 96–97.